

Klein Bound States in Single-Layer Graphene

Y. Avishai^{1,3,4} and Y. B. Band^{1,2}

¹*Department of Physics and The Ilse Katz Center for Nano-Science,
Ben-Gurion University of the Negev, Beer-Sheva, Israel.*

²*Department of Chemistry,
Ben-Gurion University of the Negev, Beer-Sheva, Israel.*

³*New-York Shanghai University,*

1555 Century Avenue, Shanghai, China.

⁴*Yukawa Institute for Theoretical Physics, Kyoto, Japan.*

(Dated: April 6, 2020)

The Klein paradox, first introduced in relation to chiral tunneling, is also manifested in the study of bound-states in single-layer graphene with a 1D square-well potential. We derive analytic (and numerical) solutions for bound-state wavefunctions, in the absence and in the presence of an external transverse magnetic field, and calculate the corresponding dipole transition rates, which can be probed by photon absorption experiments. The role of parity and time-reversal symmetries is briefly discussed. Our results are also relevant for the physics of bound states of light in periodic optical waveguide structures.

Introduction.— Chiral tunneling of electrons through a 1D potential barrier in single layer graphene was first considered in a seminal paper by Katsnelson, Novoselov, and Geim [1]. A closely related and physically motivated problem concerns the formation of electron bound states in a 1D (symmetric) potential well [2–6] (bound-states here refers to bound in one direction and free in the other direction). In this Letter we elucidate several novel aspects of such bound-states amenable to experimental verification. Our main results are: (1) In the absence of a magnetic field, bound-state eigenfunctions and eigenvalues are derived analytically, and electric dipole transition strengths are calculated to determine the absorption spectrum between bound-states. Parity and time reversal symmetry are employed to find the relation between the two (pseudo)-spinor components. (2) In the presence of an external magnetic field, analytic expressions for the bound state wavefunctions for a discrete sequence of potential strengths are derived, and are used to determine the measurable areal densities and currents. Based on ideas presented in Refs. [7, 8], our formalism also applies to the occurrence of bound states of light in periodic optical waveguide structures.

Bound states in a symmetric 1D square-well.— We search for bound states of a massless particle in single-layer graphene using the 2D Dirac equation with 1D square-well symmetric potential $U(x) = U_0\Theta(|x| - L)$. Employing L as a length unit, we define dimensionless coordinates $x \rightarrow x/L$, $y \rightarrow y/L$, potential $u(x) = LU(x)/(\hbar v_F) \equiv u_0\Theta(|x| - 1)$, energy $\varepsilon = LE/(\hbar v_F)$, (where E is the energy in physical units), and wavenumber $k = \varepsilon$, (where $E/(\hbar v_F)$ is the Fermi wavenumber in physical units). Klein physics [9] occurs for $u_0 > \varepsilon > 0$ where inside the well ($|x| < 1$) the Fermi energy lies in the conduction band while outside the well ($|x| > 1$) the Fermi energy lies in the valence band [9, 10]. Near the \mathbf{K}' Dirac point, the time-independent 2D Dirac equation (in dimensionless variables) is,

$$\mathcal{H}\Psi \equiv [-i(\sigma_x \partial_x + \sigma_y \partial_y) + u(x)]\Psi(x, y) = \varepsilon\Psi(x, y). \quad (1)$$

Under parity transformation $(x, y) \rightarrow (-x, y)$, the potential is symmetric, $u(x) = u(-x)$, but the total Hamiltonian is not, $\mathcal{H}(-x, y) \neq \mathcal{H}(x, y)$. The general solution of the wavefunction in the three different regions is, $\Psi(x, y) = e^{ik_y y} \psi(x)$,

$$\psi(x) = \begin{cases} a \begin{pmatrix} 1 \\ e^{i\phi} \end{pmatrix} e^{ik_x x} + b \begin{pmatrix} 1 \\ -e^{-i\phi} \end{pmatrix} e^{-ik_x x} & (|x| < 1), \\ \alpha \begin{pmatrix} 1 \\ -e^{i\theta} \end{pmatrix} e^{iq_x x} + \beta \begin{pmatrix} 1 \\ e^{-i\theta} \end{pmatrix} e^{-iq_x x} & (x > 1), \\ \gamma \begin{pmatrix} 1 \\ -e^{i\theta} \end{pmatrix} e^{iq_x x} + \delta \begin{pmatrix} 1 \\ e^{-i\theta} \end{pmatrix} e^{-iq_x x} & (x < -1), \end{cases} \quad (2)$$

where ϕ is the inclination angle and θ is the refractive angle. The dimensionless momentum vector inside the well [where $u(x) = 0$] is

$$\mathbf{k} = \varepsilon(\cos \phi \hat{\mathbf{x}} + \sin \phi \hat{\mathbf{y}}) \equiv k_x \hat{\mathbf{x}} + k_y \hat{\mathbf{y}}, \quad (3)$$

and $|\mathbf{k}| = \varepsilon = \sqrt{k_x^2 + k_y^2}$. The x component of the momentum outside the well [where $u(x) = u_0 > 0$] and the refractive angle are given by

$$q_x = \sqrt{(\varepsilon - u_0)^2 - k_y^2}, \\ \tan \theta = \frac{k_y}{q_x} = \frac{\varepsilon \sin \phi}{\sqrt{(\varepsilon - u_0)^2 - (\varepsilon \sin \phi)^2}}. \quad (4)$$

In the p - n - p junction analyzed here, Klein tunneling occurs for $u_0/(1 + \sin \phi) > \varepsilon > 0$ (where q_x is real), whereas Klein bound states occur for $u_0 > \varepsilon > u_0/(1 + \sin \phi) > 0$, for which

$$q_x = i\kappa_x(\varepsilon, \phi) \equiv i\sqrt{(\varepsilon \sin \phi)^2 - (u_0 - \varepsilon)^2}, \quad (5)$$

and $\kappa_x(\varepsilon, \phi) > 0$. The bound state wavefunctions must decay exponentially as $e^{-\kappa_x |x|}$ as $|x| \rightarrow \infty$. In this region $\tan \theta = -ik_y/\kappa_x$ is pure imaginary, and $\tan^2 \theta < -1$. Consequently, $\sin \theta$ is real and $\cos \theta$ is imaginary. To insure asymptotic decay at large $|x|$ we must set $\beta = \gamma = 0$ in Eq. (2). Continuity of $\psi(x)$ at $x = \pm 1$ yields a homogeneous system of four linear equations for the complex coefficient vector $\mathbf{c} \equiv (a, b, \alpha, \delta)^T$ that is an eigenvector with zero eigenvalue of the matrix $A(\varepsilon)$, $A(\varepsilon)\mathbf{c} = 0$ ($A(\varepsilon)$ is explicitly given in the Supplemental Material (SM) [11]). The determinant of $A(\varepsilon)$ is given by

$$C \det[A(\varepsilon)] = \kappa_x(\varepsilon, \phi) \cos \phi \cos(2\varepsilon \cos \phi) \\ + [\varepsilon(1 + \sin^2 \phi) - u_0] \sin(2\varepsilon \cos \phi), \quad (6)$$

where C is a non-vanishing multiplicative constant and the expression on the RHS is real. Bound-states occur at energies ε_n for which $\det[A(\varepsilon_n)] = 0$. For reasons that will be explained later, we focus on bound states at different energies $\{\varepsilon_n\}$ but for the same $k_y = \varepsilon_n \sin \phi_n$. We use the following realistic values for the parameters of graphene: $L = 172$ nm, $U_0 = 50$ meV, which yields $u_0 = \frac{LU_0}{\hbar v_F} \approx 16.0$. The pattern of bound state energies in the (ϕ, ε) plane is shown in Fig. 1(a), together with the curve $k_y = \varepsilon \sin \phi = 10$ ($= 0.0581$ nm⁻¹). The intersection points indicate bound-state energies $\{\varepsilon_n\}$ with the same value of $k_y = \varepsilon_n \sin \phi_n$.

Bound state wavefunctions.— Now we compute the wavefunctions for (ε_n, ϕ_n) , $n = 0, 1, \dots, 7$, see Fig. 1(a). The pairs (ε_n, ϕ_n) are inserted into the matrix A and the spinor bound-state wavefunctions

$\psi_n(x) = \begin{pmatrix} \psi_n^{(1)} \\ \psi_n^{(2)} \end{pmatrix}$ are determined in terms of the four coefficients $\mathbf{c}_n \equiv (a_n, b_n, \alpha_n, \delta_n)$, i.e., the solution of the eigenvalue equation $A(\varepsilon_n, \phi_n)\mathbf{c}_n^T = 0$. Due to parity symmetry (see below), the components of the spinors are subject to the constraints,

$$\begin{aligned} \text{Im}[\psi_n^{(1)}(x)] &= \text{Re}[\psi_n^{(2)}(x)] = 0, \\ \text{Im}[\psi_n^{(2)}(x)] &= (-1)^n \text{Re}[\psi_n^{(1)}(-x)]. \end{aligned} \quad (7)$$

Analytic expressions for the ground and excited state wavefunctions are derived by choosing

$$a = b^* = \mathcal{A}_n e^{i\eta_n}, \quad \eta_n = (2n+1)\frac{\pi}{4} - \frac{1}{2}\phi. \quad (8)$$

where \mathcal{A}_n are real normalization constants and the phase η_n is chosen to satisfy the symmetries in Eq. (7). Combining Eqs. (2) and (8), the bound-state wavefunctions, $\Psi_n(x, y) = e^{ik_y y} \psi_n(x)$ for $|x| < 1$ are,

$$\begin{aligned} \psi_n(x, y) &= \mathcal{A}_n \begin{pmatrix} \psi_n^{(1)}(x) \\ (-1)^n i \psi_n^{(1)}(-x) \end{pmatrix} \\ &= \mathcal{A}_n \begin{pmatrix} \cos[\gamma_n^-(x)] + \sin[\gamma_n^-(x)] \\ (-1)^n i \{\cos[\gamma_n^+(x)] + \sin[\gamma_n^+(x)]\} \end{pmatrix}, \quad (9) \\ \gamma_n^\pm(x) &= \frac{1}{2}(\phi_n \pm 2k_{nx}x), \end{aligned}$$

where $k_{nx} = \varepsilon_n \cos \phi_n$. The decaying parts of the wavefunctions for $|x| > 1$ are determined by the coefficients β, δ , and the symmetry specified in Eq. (7) is fulfilled for all x . The two upper components of the spinor wavefunctions $\psi_{n=0,1}(x)$ are shown in Fig. 1(b).

The symmetry specified in Eq. (7) also implies that $\psi_0^\dagger(x)\psi_1(x)$ is an odd function of x . Hence, $\langle \psi_0 | \psi_1 \rangle = 0$, i.e., the two states are orthogonal, as are any two different eigenfunctions.

Currents.— Bound states, with wavefunctions $\psi_n(x) = \begin{pmatrix} \psi_n^{(1)}(x) \\ \pm i \psi_n^{(1)}(-x) \end{pmatrix}$, do not carry current along x : $J_{nx}(x) \equiv \psi_n^\dagger(x) \sigma_x \psi_n(x) = 0$. However, they do carry current along y , $J_{ny}(x) \equiv \psi_n^\dagger(x) \sigma_y \psi_n(x) \neq 0$, ($n = 0, 1$), that is symmetric under $x \leftrightarrow -x$ and it quickly decays for $|x| > 1$. As we discuss below in connection with time reversal invariance, all states are Kramers degenerate, and the two degenerate states forming a Kramers pair carry currents in opposite directions.

Parity.— The importance of parity in the physics of graphene is discussed in Ref. [12], where it is shown that parity operator in (1+2) dimensions plays an interesting role and can be used for defining conserved chiral currents (see also Ref. [15]). Here we concentrate on bound states, wherein the current along x should vanish, and consider the role of the parity transformation under which the Hamiltonian is *not* invariant. For a symmetric potential, $u(x) = u(-x)$, we consider the static (time-independent) case with Hamiltonian $\mathcal{H}(x, y)$ introduced in Eq. (1). The parity transformation in 2+1 dimensions is taken to mean the transformation $(x, y) \rightarrow (-x, y)$. For massless Dirac fermions this transformation is realized by the operator σ_y . Explicitly,

$$\begin{aligned} \mathcal{H}^P(x, y) &\equiv \sigma_y \mathcal{H}(x, y) \sigma_y = i\sigma_x \partial_x - i\sigma_y \partial_y + u(x) \\ &= \mathcal{H}(-x, y) \neq \mathcal{H}(x, y). \end{aligned} \quad (10)$$

Thus, near a given Dirac point, say \mathbf{K}' , \mathcal{H} is not parity invariant [despite the fact that $u(x) = u(-x)$] [18]. However, for a symmetric potential the wavefunctions $\psi_n(x)$ in Eq. (9) obey the symmetry relations,

$$\sigma_y \psi_0(x) = \psi_0(-x), \quad \sigma_y \psi_1(x) = -\psi_1(-x). \quad (11)$$

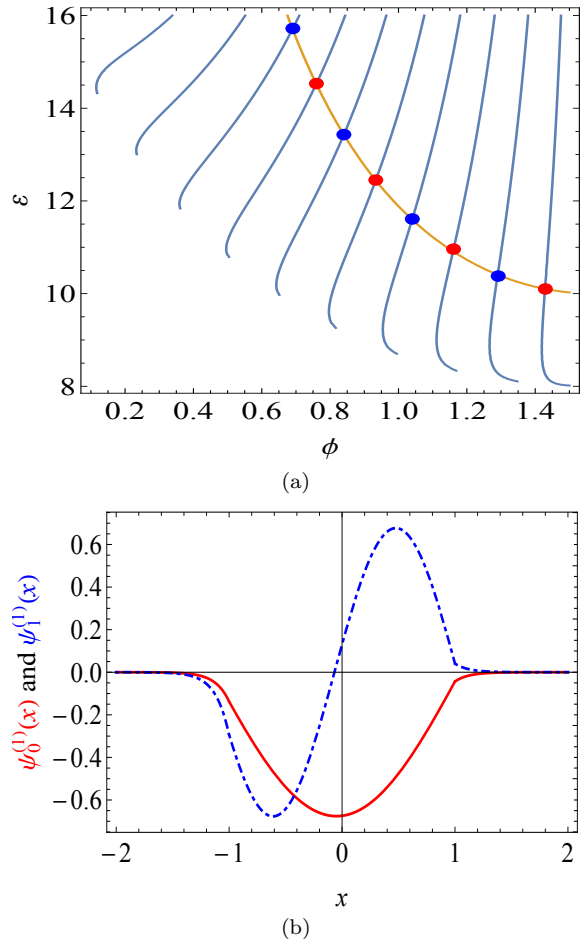


FIG. 1: (a) Nodes of $\det[A(\varepsilon, \phi)]$, Eq. (6), in the (ϕ, ε) plane (blue curves), and the curve $k_y = \varepsilon \sin \phi = 10$ (orange curve). The pairs (ε_n, ϕ_n) specified by blue and red dots are the bound state energies for $k_y = \varepsilon_n \sin \phi_n = 10$. (b) Upper components of $\psi_0(x)$ (red solid curve) and $\psi_1(x)$ (blue dot-dashed curve) versus x . The lower components are related to the upper ones via Eq. (9). Note that the wavefunctions do not have a definite symmetry around $x = 0$ (see discussion on the role of parity below).

Equation (11) is a concrete realization of Eq. (14) in Ref. [12]. Hence, we define $\psi_n(x)$ as being $\begin{pmatrix} \text{even} \\ \text{odd} \end{pmatrix}$ under parity if and only if $\sigma_y \psi(x) = \pm \psi(-x)$. With this assignment, Eq. (11) is consistent with (albeit different than) the non-relativistic one-dimensional problem, where, in a symmetric potential, the parity of eigenstates is such that $\psi_n(-x) = (-1)^n \psi_n(x)$, $n = 0, 1, 2, \dots$, and the ground-state is symmetric. By definition,

$$\mathcal{H}\psi_n(x) = \varepsilon_n \psi_n(x) \Rightarrow \mathcal{H}^P \psi_n(-x) = \varepsilon_n \psi_n(-x). \quad (12)$$

Thus, $\psi_n(x)$ and $\psi_n(-x) \neq \pm \psi_n(x)$ are respectively eigenfunctions of \mathcal{H} and $\mathcal{H}^P \neq \mathcal{H}$ with the same eigenvalue ε_n .

Time Reversal Invariance.— The time reversal operator is $\mathcal{T} = i\sigma_y K$, where K is the complex conjugation operator. It is easy to check that $[\mathcal{H}, \mathcal{T}] = 0$, so that each state is doubly (Kramers) degenerate. Applying the operator \mathcal{T} on a wavefunctions $\Psi_n(x, y)$, Eq. (9) we obtain [recall that $\psi_n^{(1)}(x)$ is real and $\psi_n^{(2)}(x) = (-1)^n i \psi_n^{(1)}(-x)$ is purely imaginary],

$$\Psi_n^{\mathcal{T}}(x, y) = \mathcal{A}_n e^{-ik_y y} \begin{pmatrix} (-1)^n \psi_n^{(1)}(-x) \\ i \psi_n^{(1)}(x) \end{pmatrix}, \quad (13)$$

which is the Kramers partner of $\Psi_n(x, y)$, i.e., $\mathcal{H}\Psi_n^{\mathcal{T}}(x, y) = \varepsilon_n \Psi_n^{\mathcal{T}}(x, y)$.

Electromagnetic Transitions.— Consider $E1$ transitions induced by x polarized light such that the dipole operator is $\mathcal{O}(x) = eE_x x$, where E_x is the

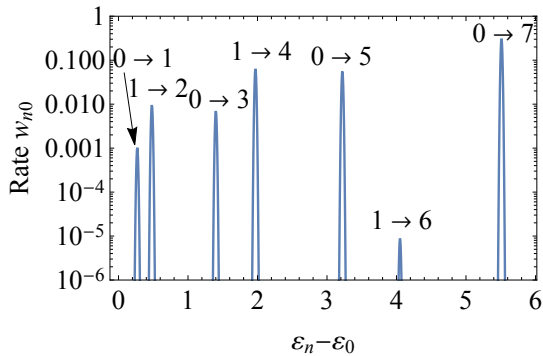


FIG. 2: Absorption spectrum of the transitions $0 \rightarrow 1$, $0 \rightarrow 3$, $0 \rightarrow 5$, $0 \rightarrow 7$, $1 \rightarrow 2$, $1 \rightarrow 4$, $1 \rightarrow 6$. The absorption rate w_{nm} (in dimensionless units) from level n to level m is plotted as a function of the resonant absorption photon energy $\hbar\omega_{nm} = \varepsilon_n - \varepsilon_m$ (in dimensionless units).

electric field amplitude. The parity of the product $\psi_n^\dagger(x)\psi_m(x)$ is $(-1)^{n+m+1}$. Because k_y is conserved and is the same for $\Psi_n(x, y)$ and $\Psi_m(x, y)$, we have,

$$\langle \Psi_m | \mathcal{O} | \Psi_n \rangle = \frac{1}{2} [1 - (-1)^{n+m}] e E_x \langle x \rangle_{n,m}. \quad (14)$$

Figure 2 shows the absorption spectrum of the transitions $0 \rightarrow 1$, $1 \rightarrow 2$, $0 \rightarrow 3$, $1 \rightarrow 4$, $0 \rightarrow 5$, $1 \rightarrow 6$, $0 \rightarrow 7$, where the absorption rates (in arbitrary units) w_{nm} from m to n are proportional to $\omega_{nm}^4 |\langle \psi_n | x | \psi_m \rangle|^2$ where $\hbar\omega_{nm} = \varepsilon_n - \varepsilon_m$ [13].

Strictly speaking, electrons can occupy orbits with arbitrary $k_y < \varepsilon$ and transitions can occur between the pertinent energy states. However, practically, an experiment can be carried out in a graphene nano-ribbon of width L_y such that $k_y = \frac{2\pi p}{L_y}$, ($p = 1, 2, \dots$) is quantized. If L_y is small enough, only the lowest mode is occupied. In our example, $k_y = 10$ and $\varepsilon < u_0 = 16$ (in dimensionless units). If this value of k_y corresponds to the lowest mode $p = 1$, then the second mode ($p = 2$) has $k_y = 20 > \varepsilon$. In physical units, this implies $k_y = 0.058 \text{ nm}^{-1}$ and $L_y = 108 \text{ nm}$. Experimental fabrications of much lower nano-ribbon width have already been reported [14].

Bound States in a perpendicular magnetic field and square well.— Analysis of bound states in the presence of uniform perpendicular magnetic field and a square well potential enables an access to “unquantized” Landau functions in graphene. First recall the extensively studied case $U(x) = 0$ (see *e.g.*, Ref. [16]). In the Landau gauge, $A_y = Bx$, the spinor wavefunction is $\Psi(x, y) = e^{ik_y y} \psi(x)$. Introducing the magnetic length $\ell = \sqrt{\hbar c / (eB)}$ enables formulation in terms of the dimensionless position, wave number and binding energy: $x \rightarrow x/\ell$, $k_{x,y} \rightarrow k_{x,y}\ell$ and $\varepsilon = \frac{\ell E}{\hbar v_F}$. The bare equation with dimensionless variables and parameters then reads, $[-i\sigma_x \partial_x + \sigma_y (k_y - x)]\psi(x) = \varepsilon\psi(x)$. It is simplified after a shift and scaling of the position coordinate, $x \rightarrow \frac{z}{\sqrt{2}} + k_y$,

$$\mathcal{H}\psi(z) \equiv [-i\sigma_x \partial_z - \frac{1}{2}z\sigma_y]\psi(z) = \varepsilon\psi(z), \quad (15)$$

whose general solution is (with $\bar{\delta} \equiv 1 - \delta$),

$$\begin{pmatrix} \psi^{(1)}(z) \\ \psi^{(2)}(z) \end{pmatrix} = c_1 \begin{pmatrix} D_{\nu_1}(z) \\ \frac{\varepsilon}{i} D_{\nu_1-1}(z) \end{pmatrix} + c_2 \bar{\delta}_{\varepsilon,0} \begin{pmatrix} D_{\nu_2}(iz) \\ \frac{-1}{\varepsilon} D_{\nu_2+1}(iz) \end{pmatrix} \quad (16)$$

where $D_\nu(z)$ is the parabolic cylinder function, $z \equiv z(x) = \sqrt{2}(x - k_y)$, $\nu_1 = \varepsilon^2$, $\nu_2 = -(\varepsilon^2 + 1)$. If the wavefunction is required to be square integrable on the whole interval $-\infty < z < \infty$, we must set $\varepsilon^2 = n$, (where n is a non-negative integer), and $c_2 = 0$ (because wavefunctions with imaginary arguments

blow up). These constraints determine the Landau quantized energies $\varepsilon = \pm\sqrt{n}$ and wavefunctions for electrons in graphene.

In the scaled shifted variable z the square-well potential $U(x) = U_0\Theta(|x| - L)$ reads,

$$u(z) = \begin{cases} 0, & z(-L) < z < z(L) \\ u_0, & \text{otherwise} \end{cases}, \quad (17)$$

where $u_0 = \frac{\ell U_0}{\hbar v_F}$ and $z(L) = \sqrt{2}L - k_y \equiv L_1$, $z(-L) = -\sqrt{2}L - k_y \equiv L_2 \neq -z(L) = -L_1$, hence $k_y = -\frac{1}{2}[z(L) + z(-L)]$. Thus, a symmetric well in x is not symmetric in z . The eigenvalue problem is specified by the set of equations defined for $-\infty < z < \infty$,

$$[-i\sigma_x \frac{d}{dz} - \frac{1}{2}z\sigma_y]\psi(z) = \begin{cases} \varepsilon\psi(z), & z \in [L_2, L_1] \\ (\varepsilon - u_0)\psi(z), & z \notin [L_2, L_1]. \end{cases} \quad (18)$$

Here $\psi(z) = \begin{pmatrix} \psi^{(1)}(z) \\ \psi^{(2)}(z) \end{pmatrix}$, and ε is the energy eigenvalue that needs to be determined. As in Eq. (16), the solutions can be expressed in terms of parabolic cylinder functions $D_\nu(\cdot)$, and the spinor wavefunction is required to be continuous everywhere and square-integrable. For $z \in [L_2, L_1]$ the solution reads,

$$\psi_c(z) = c_1 \begin{pmatrix} D_{\nu_1}(z) \\ -i\varepsilon D_{\nu_1-1}(z) \end{pmatrix} + c_2 \bar{\delta}_{\varepsilon,0} \begin{pmatrix} D_{\nu_2}(iz) \\ -\frac{1}{\varepsilon} D_{\nu_2+1}(iz) \end{pmatrix} \quad (19)$$

Generically, the orders $\nu_1 = \varepsilon^2$, $\nu_2 = -(\varepsilon^2 + 1)$ in Eq. (19) are not (non-negative) integers. In the external regions $z \notin [L_2, L_1]$, the only solutions of the second of Eq. (18) that decay as $|z| \rightarrow \infty$ are such that: (1) the order ν of $D_\nu(\cdot)$ should be a non-negative integer, and (2) the argument of $D_\nu(\cdot)$ must be real. The most general solution is then an infinite linear combination of Landau functions $L_{sn}(z) = \begin{pmatrix} D_n(z) \\ s i \sqrt{n} D_{n-1}(z) \end{pmatrix}$, $n = 0, 1, \dots$, $s = \mp$. A general numerical solution is worked out in the supplemental material[11]. Here we show that analytic solutions exist for specific discrete values of the potential strength u_0 . We employ the following solutions of Eq. (18) for $z \notin [L_2, L_1]$, with $\varepsilon = u_0 \pm \sqrt{n}$, that is, $n = (\varepsilon - u_0)^2$:

$$\begin{aligned} \psi_{\text{right}}(z) &= c_3 \Theta(z - L_1) \begin{pmatrix} D_n(z), \\ \pm i \sqrt{n} D_{n-1}(z) \end{pmatrix}, \\ \psi_{\text{left}}(z) &= c_4 \Theta(L_2 - z) \begin{pmatrix} D_n(z) \\ \pm i \sqrt{n} D_{n-1}(z) \end{pmatrix}. \end{aligned} \quad (20)$$

Matching Equations.— Following Eqs. (19) and (20), for fixed $\pm\sqrt{n}$, the wavefunction is determined by the coefficients vector $\mathbf{c} = (c_1, c_2, c_3, c_4)^T$. Continuity requires $\psi_c(L_1) = \psi_{\text{right}}(L_1)$ and $\psi_c(L_2) = \psi_{\text{left}}(L_2)$, where each relation yields two equations. This set of four linear homogeneous equations can be formally written as $A_n(u_0)\mathbf{c} = 0$. The potential strength u_0 must satisfy $\text{Det}[A_n(u_0)] = 0$, and the roots u_{nm} determine the bound-state energies $\varepsilon_{nm} = u_{nm} \pm \sqrt{n}$. The eigenvector \mathbf{c}_{nm} of $A_n(u_{nm})$ corresponding to eigenvalue zero determines the wavefunction in all space. Figure 3(a) plots $\text{Det}[A_n(u_0)]$ versus u_0 . For each $0 \leq n \in \mathbb{Z}$ there are, in principle, an infinite number of zeros $\{u_{nm}\}$ and infinite number of bound-state energies $\varepsilon_{nms} = u_{nm} + s\sqrt{n}$, where $s = \pm$. A few bound state energies are shown in Fig. 3(b).

Wavefunctions and Currents.— The spinor wavefunctions and the currents along y corresponding to well height u_{nm} for $(n, m) = (0, 0)$ are shown in Fig. 4. The main properties of the wavefunctions are: (1) It is possible to choose the phase such that the upper component of the spinor is real while the

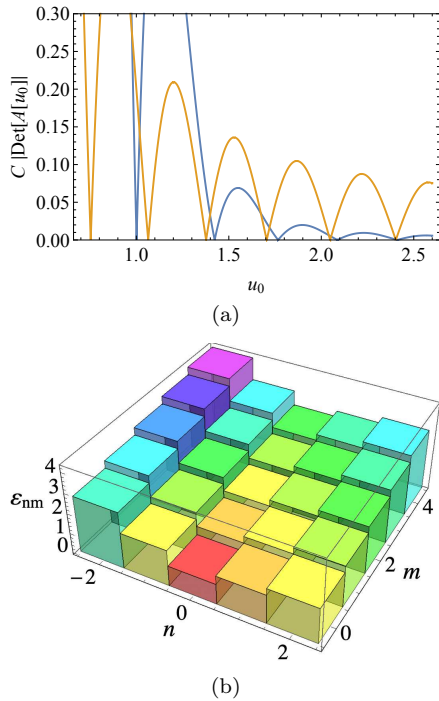


FIG. 3: (a) For square well boundary conditions with $L_2 = -3.1\sqrt{2}$ and $L_1 = 2.1\sqrt{2}$ (in units of ℓ) we plot $|\text{Det}[A_n(u_0)]|$ as function of u_0 for $n = 0$ (blue) and $n = 1$ (orange). The zeroes u_{nm} fix the bound-state energies, $\epsilon_{nm} = u_{nm} \pm \sqrt{n}$, $n = 0, 1, 2, \dots$, $m = 0, 1, 2, \dots$ (b) 3D discrete plot of the bound-state energies ϵ_{nm} (negative n means $\epsilon_{nm} = u_{nm} - \sqrt{n}$). The points (n, m, ϵ_{nm}) are the center of a unit square placates with half integer vertices, $(n \pm 1/2, m \pm 1/2)$. The square placates are drawn simply to graphically clarify the values of ϵ_{nm} .

lower component is imaginary. This implies that the current along x vanishes, as it should for bound states. (2) Parity symmetry (or antisymmetry) is not exact for the wave functions around $z = 0$. The density $\rho(z) = \psi_0^\dagger(z)\psi_0(z)$ is not perfectly symmetric and the current density $J_y(z) = \psi_0^\dagger(z)\sigma_y\psi_0(z)$ is not perfectly antisymmetric, hence the total (integrated) current I_y does not vanish. (With the particular choice of parameters adopted here we get $I_y = 0.00737326$). The reason for this is that the energy levels are degenerate $\epsilon(k_y) = \epsilon(-k_y)$ and the corresponding quantities for $\pm k_y$ are related:

$$\rho(z; -k_y) = \rho(-z; k_y), \quad J_y(z; -k_y) = -J_y(-z; k_y). \quad (21)$$

Hence, the (incoherent) weighted sums of contributions from $\pm k_y$ satisfy the pertinent symmetries, and hence $I_y = 0$ for the weighted sums. In principle, $\rho(z)$ and $J_y(z)$ can be measured together with dipole transition rates (see discussion and illustration in the SM [11]). Therefore, graphene Landau wavefunctions with non-integer orders can be probed.

Summary and Conclusions.— We have developed a formalism for studying electron Klein bound states in single layer graphene subject to a symmetric 1D square-well potential, in the absence as well as in the presence of an external magnetic field. This study completes and adds novel concepts to the analysis of chiral tunneling reported Ref. [1]. In the absence of magnetic field, an analytic expression is derived for the wavefunctions of the ground and excited states, and a beautiful symmetry between the two components of the (pseudo-)spinor is ex-

posed. The consequences of parity non-invariance and time reversal invariance are elucidated, and photon absorption inducing $E1$ transition between two levels is worked out. In the presence of an external uniform perpendicular magnetic field, an analytic expression for the wavefunctions is derived

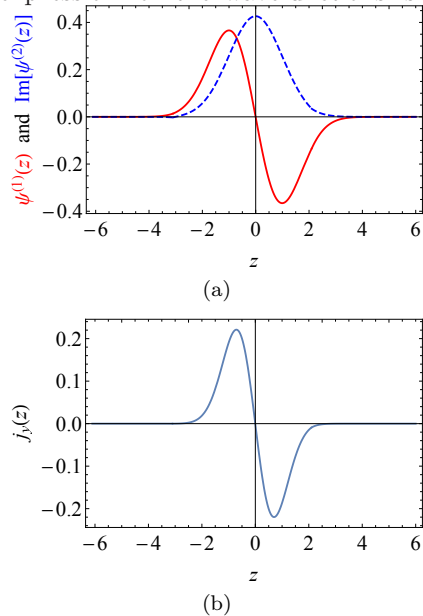


FIG. 4: For the potential strength $u_0 = u_{n=0, m=0} = 1.0013$ [the first blue zero in Fig. 3(a)] and width $L_2 = -3.1\sqrt{2}$, $L_1 = 2.5\sqrt{2}$ we plot (a) the upper component (red) and $-i$ times the lower component (blue) of the wavefunction $\psi_{10}(z)$, and (b) the current $J_y(z)$ of the state $\psi_{00}(z)$. Since u_{00} is small, the wave functions and current seem to have perfect symmetry around $z = 0$ but, strictly speaking, they are not (see discussion in the text and Ref.[11]).

for a discrete (albeit infinite) sequence of potential strengths $u_0 = \{u_{nm}\}$ $n, m = 0, 1, 2, \dots$. The Landau functions (in graphene) with non-integer orders and imaginary argument appearing in Eq. (19) are thereby exposed to experimental probes. Exact numerical calculations valid for every potential strength are carried out in the supplemental material [11], and the importance of the symmetry (21) is stressed.

Our results apply directly to the propagation of light waves in periodic waveguide optical structures. Transport of light in a 2D binary photonic superlattice with two interleaved lattices A and B is realized by a sequence of equally spaced waveguides with alternating deep/shallow peak refractive index changes. Propagation of monochromatic light waves is well-described by the scalar wave equation in the paraxial approximation. The tight-binding limit results in coupled-mode equations for the fundamental-mode field amplitudes which are functions of a discrete set of integer variables, and approximating these with a continuous variable rather than as an integer index yields a 2D Dirac equation with an external electrostatic potential [7, 8]. This yields the same mathematical formalism used to describe graphene.

Acknowledgments: We would like to thank Mikhail I. Katsnelson, Jean Noël Fuchs Ken Shiozaki and Ady Stern for illuminating discussions. This work was supported in part by a grant from the DFG through the DIP program (FO703/2-1).

[1] M. I. Katsnelson, K. S. Novoselov, and A. K. Geim, Nature Physics **2**, 620 (2006).

[2] J. M. Pereira Jr., V. Mlinar, F. M. Peeters, P. Vasilopoulos, Phys. Rev. B **74**, 045424 (2006).

- [3] M. Ramezani Masir, P Vasilopoulos and F. M. Peeters, *New Journal of Physics*, **11**, (2009).
- [4] M. Barbier, P. Vasilopoulos and F. M. Peeters, *Phil. Trans. R. Soc. A* **368**, 5499 (2010).
- [5] H. C. Nguyen, M. T. Hoang, and V. L. Nguyen, *Phys. Rev. B* **79**, 035411 (2009).
- [6] C. Gutiérrez, L. Brown, C-J Kim, J. Park and A. N. Pasupathy, *Nature Phys.* **12**, 1069, (2016).
- [7] S. Longhi, *Phys. Rev. B* **81**, 075102 (2010).
- [8] S. Longhi, *Appl. Phys. B* **104**, 453-468 (2011).
- [9] O. Klein, *Zeitschrift für Physik*, 53, 157 (1929), https://en.wikipedia.org/wiki/Klein_paradox.
- [10] Pierre E. Allain and Jean-Noël Fuchs, *Eur. Phys. J. B* **83**, 301 (2011).
- [11] See the Supplemental Materials, <http://xxx>.
- [12] Riazuddin, “Dirac equation for quasi-particles in graphene in an external electromagnetic field and chiral anomaly”, arXiv:1105.5956.
- [13] Y. B. Band and Y. Avishai, *Quantum Mechanics, with Applications to Nanotechnology and Quantum Information Science*, (Academic Press – Elsevier, 2013), Sec. 7.9.4.
- [14] V. Barone and O. Hod *et al*, *Nano Letters* **6**, No.12 (2006).
- [15] E. Sadurni, *Revista Mexicana de Fisica* **61**, 170-181 (2015).
- [16] Z. Lenarcic, *Landau Levels in Graphene*, http://www-f1.ijs.si/~ramsak/Nanofizika/grafen/zala_lenarcic_grafen.pdf
- [17] F. W. J. Olver, *Uniform Asymptotic Expansions for Weber Parabolic Cylinder Functions of Large Orders*, *Journal of Research of the National Bureau of Standards B. Mathematics and Mathematical Physics*, **63B**, No.2, October-December 1959.
- [18] The reason is that there are two inequivalent representations of the 2D Dirac γ matrices. Parity operation carries valley $\mathbf{K} \rightarrow \mathbf{K}'$, and its conservation can be restored if valley degeneracy is incorporated in the Lagrangian, when it is built upon both representations [12].

Supplemental Material for “Klein Bound States in Single-Layer Graphene”

Y. Avishai^{1,3,4} and Y. B. Band^{1,2}

¹*Department of Physics and The Ilse Katz Center for Nano-Science,
Ben-Gurion University of the Negev, Beer-Sheva, Israel.*

²*Department of Chemistry,
Ben-Gurion University of the Negev, Beer-Sheva, Israel.*

³*New-York Shanghai University,
1555 Century Avenue, Shanghai, China.*

⁴*Yukawa Institute for Theoretical Physics, Kyoto, Japan.*

Here we elaborate on several points discussed in the main text (MT) [1]. Section I contains additional information regarding the matrix $A(\varepsilon)$ introduced in Eq. (6) of the MT. Section II considers the numerical solution of Eq. (18) in the MT, and Sec. III discusses the electric dipole (E_1) transitions between bound states.

I. THE MATRIX $A(\varepsilon)$ RELATED TO EQ. (6)

In this section we give an explicit expression for the matrix $A(\varepsilon)$ that determines the bound state energies and wavefunction coefficients specified by the vector $\mathbf{c} \equiv (a, b, \alpha, \delta)$ appearing in Eq. (2). The pertinent quantities are introduced in the discussion near Eqs. (3), (4), and (5) in the MT. The matching conditions at $x = \pm 1$ lead to a homogeneous system of four linear equations for the complex coefficients a, b, α, δ . Bound-state solutions occur at energies $\{\varepsilon_n\}$ for which the determinant of $A(\varepsilon)$ vanishes, and the corresponding coefficient vector \mathbf{c}_n is determined by the set of homogeneous equations $A(\varepsilon_n)\mathbf{c}_n = 0$. The explicit form of the matrix $A(\varepsilon)$ in the system of equations, $A(\varepsilon)\mathbf{c} = 0$, is given by

$$A(\varepsilon) = \begin{pmatrix} e^{i\varepsilon \cos \phi} & e^{-i\varepsilon \cos \phi} & -e^{-\kappa_x} & 0 \\ e^{i(\varepsilon \cos \phi + \phi)} & -e^{-i(\varepsilon \cos \phi + \phi)} & e^{(-\kappa_x + i\theta)} & 0 \\ e^{-i\varepsilon \cos \phi} & e^{i\varepsilon \cos \phi} & 0 & -e^{-\kappa_x} \\ e^{-i(\varepsilon \cos \phi - \phi)} & -e^{i(\varepsilon \cos \phi - \phi)} & 0 & -e^{(-\kappa_x - i\theta)} \end{pmatrix}. \quad (1)$$

II. NUMERICAL SOLUTION OF EQ. (18)

The set of Landau functions is complete on the interval $(-\infty, \infty)$ so we can expand $\psi(z)$:

$$\psi(z) = \sum_{n=0}^{M \rightarrow \infty} \sum_{s=\mp} a_{ns} L_{ns}(z), \quad \text{where } L_{ns}(z) = N_{ns} \begin{pmatrix} D_n(z), \\ si\sqrt{n}D_{n-1}(z) \end{pmatrix}, \quad (2)$$

Here N_{ns} is a normalization factor. Substitution into Eq. (18) then yields,

$$[-i\sigma_x \partial_z - \frac{1}{2}z\sigma_y]\psi(z) = \sum_{n=0}^M \sum_{s=\mp} a_{ns} s\sqrt{n}L_{ns}(z) = [\varepsilon - u(z)] \sum_{n=0}^M \sum_{s=\mp} a_{ns} L_{ns}(z). \quad (3)$$

Multiplying by $L_{mt}^\dagger(z)$ (where $t = \mp$) and integrating over z , using $\langle L_{mt} | L_{ns} \rangle = \delta_{mn}\delta_{ts}$ one obtains,

$$t\sqrt{m}a_{mt} = \varepsilon a_{mt} - \sum_{n=0}^M \sum_{s=\pm} A_{mt,ns} a_{ns}. \quad (4)$$

The infinite sum (as $M \rightarrow \infty$) can be cut-off at a sufficiently large M . This procedure leads to an eigenvalue problem in a finite Hilbert space of dimension $2M + 1$. The matrix A introduced above can be written as $u_0(I - B)$, where I is the $(2M + 1) \times (2M + 1)$ unit matrix. The explicit expressions for the matrices A and B are,

$$A_{mt,ns} = \int_{-\infty}^{\infty} L_{mt}^\dagger(z) u(z) L_{ns}(z) dz = u_0 \underbrace{[\delta_{mn}\delta_{ts}]}_{I_{mt,ns}} - \underbrace{\int_{L_2}^{L_1} L_{mt}^\dagger(z) L_{ns}(z) dz}_{B_{mt,ns}}. \quad (5)$$

where u_0 is the strength of the square well potential defined in Eq. (17) in the MT. Next, we define a diagonal matrix Λ by

$$\Lambda_{mt,ns} = \delta_{mt,ns} \text{Diag}(t\sqrt{m}) = (0, \sqrt{1}, \sqrt{2}, \dots, \sqrt{M}, -\sqrt{1}, -\sqrt{2}, \dots, -\sqrt{M}), \quad (6)$$

and a vector \mathbf{a} with $2M + 1$ components, $a_{ns} = (a_0, a_{1+}, a_{2+}, \dots, a_{M+}, a_{1-}, a_{2-}, \dots, a_{M-})$. Equation (4) then becomes an eigenvalue problem,

$$[\Lambda + u_0(I - B)]\mathbf{a} = \varepsilon \mathbf{a}, \quad (7)$$

The matrix $\Lambda + u_0(I - B)$ is real and symmetric. For $u_0 = 0$ the eigenvalues are the Landau energies for graphene $\varepsilon_m = \pm\sqrt{m}$. In the calculations of density, current and E_1 transitions presented below we take

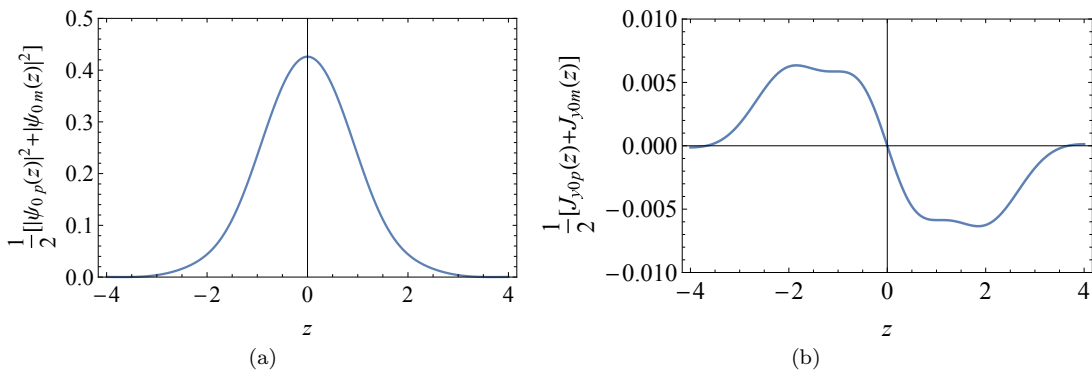


FIG. 1: Density $\rho_0(z)$ and current $J_{y0}(z)$ of the ground state $\psi_0(z)$ following incoherent summation over $\pm k_y$. (a) $\frac{1}{2}[\rho_0(z, k_y) + \rho_0(z, -k_y)]$, (b) $\frac{1}{2}[J_{y0}(z, k_y) + J_{y0}(z, -k_y)]$.

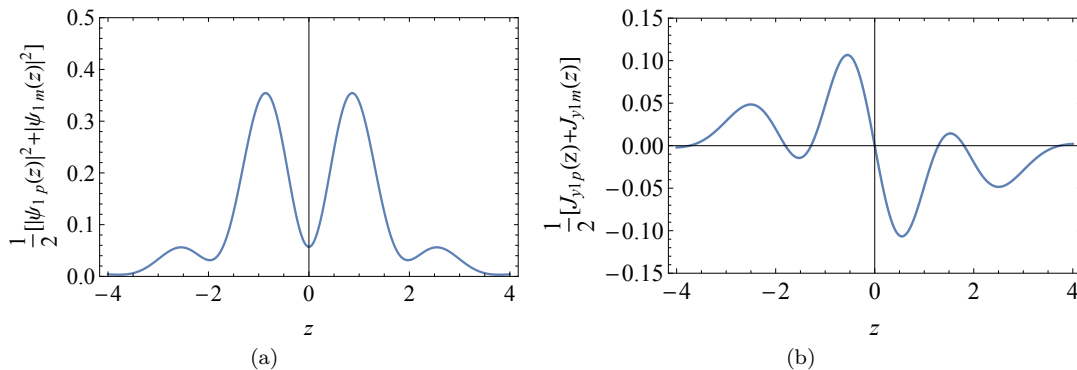


FIG. 2: Density $\rho_1(z)$ and current $J_{y1}(z)$ of the first excited state $\psi_1(z)$ following incoherent summation over $\pm k_y$. (a) $\frac{1}{2}[\rho_1(z, k_y) + \rho_1(z, -k_y)]$, (b) $\frac{1}{2}[J_{y1}(z, k_y) + J_{y1}(z, -k_y)]$.

$u_0 = \frac{\ell U_0}{\hbar v_F} = 10$, $-\frac{5}{2\sqrt{2}} \leq x \leq \frac{5}{2\sqrt{2}}$ (in units of ℓ), and $k_y = \pm 0.5$ (in units of $1/\ell$). Since $z = \sqrt{2}x - k_y$, this gives $[L_2, L_1] = [-3, 2]$ for $k_y = +0.5$, and $[L_2, L_1] = [-2, 3]$ for $k_y = -0.5$.

Figure 1 shows the ground-state density symmetrized density $\rho_0(z) = \frac{1}{2} \sum_{\pm k_y} [\psi_0^\dagger(z)\psi_0(z)]$ and current density along y , $J_{y0}(z) = \frac{1}{2} \sum_{\pm k_y} [\psi_0^\dagger(z)\sigma_y\psi_0(z)]$. As argued in the discussion of Eq. (21) of the MT, the incoherent sum of contributions from $\pm k_y$ results in a symmetric density and an antisymmetric current density. In particular, the total current along y , $I_{y0} = \int_{-\infty}^{\infty} J_{y0}(z)dz$ vanishes (as it should). Similar results for the first excited state $\psi_1(x)$ are shown in Fig. 2.

III. E_1 TRANSITIONS IN THE PRESENCE OF MAGNETIC FIELD

In analogy with the discussion of photon absorption in the absence of an external magnetic field [see Eq. (14) in the MT], we now consider E_1 transitions in the presence of the magnetic field. The E_1 transition rates $w_{n,m}$ from m to n with light polarized along the x axis are proportional to $|\varepsilon_n - \varepsilon_m|^4 |\langle \psi_n | x | \psi_m \rangle|^2$, where $\{\varepsilon_n\}$ are the energy eigenvalues obtained from the solution of Eq. (7) and the transition dipole matrix elements are

$$\langle x \rangle_{mn} = \langle \psi_m | x | \psi_n \rangle = \int_{-\infty}^{\infty} \psi_m^\dagger[z(x)]x\psi_n[z(x)]dx, \quad (8)$$

where $z(x) = \sqrt{2}(x - k_y)$. The main contribution comes from the interval $-L \leq x \leq L$ where $L/\ell = \frac{5}{2\sqrt{2}}$ [see details below Eq. (7)]. Photon absorption spectrum between the lowest eight states $n = 0, 1, \dots, 7$ [determined within the set of parameters specified after Eq. (7)], is shown in Fig. 3. It is interesting to underline the differences between photon absorption spectra in the presence and in the absence of the magnetic field shown in Fig. 2 in the MT. In the latter case, there is the usual parity selection rule, namely, the function $\psi_n^\dagger(x)x\psi_m(x)$ is even (odd) if $n + m + 1$ is odd (even). In particular, transitions $0 \rightarrow 1, 3, 5, 7$ are shown but $0 \rightarrow 2, 4, 6$ vanish. These parity selection rules do not apply in the presence of magnetic field, hence all transitions $0 \rightarrow n$ ($n = 1, 2, \dots, 7$) are allowed.

One can easily convert the E_1 transition rates to physical units. Following Ref. [2] (p. 324), the E_1 transition rate between states $|m\rangle$ and $|n\rangle$ is given, (up to a multiplicative factor A depending on constants such as c and \hbar), by:

$$w_{mn} = A(E_m - E_n)^4 (e\mathcal{E}_x)^2 |X_{mn}|^2, \quad X_{mn} = \langle m | x | n \rangle,$$

where E_m and E_n are the level energies and \mathcal{E}_x is the slowly varying envelope of the electric field. The physical dimension of w_{mn} is $[w_{mn}] = [A] \times [\text{energy}]^6$. If there is a parameter of length d in the system, then we can use it as the unit of length and work with dimensionless quantities: ε_m for energy E_m , u_0 for potential height U_0 , $k_y \rightarrow k_y d$ for wave numbers and x_{mn} for X_{mn} :

$$E_m = \frac{\hbar v_F}{d} \varepsilon_m, \quad U_0 = \frac{\hbar v_F}{d} u_0, \quad X_{mn} = dx_{mn}, \quad \Rightarrow w_{mn} = A \left[\frac{\hbar v_F}{L} \right]^4 (\varepsilon_n - \varepsilon_m)^4 (e\mathcal{E}_x d)^2 |x_{mn}|^2.$$

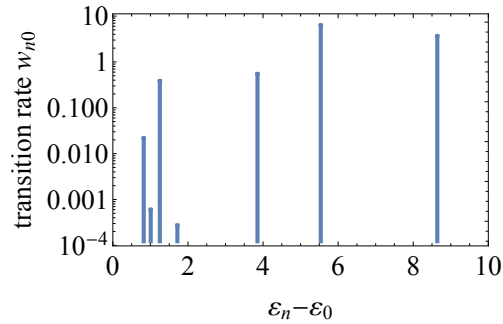


FIG. 3: Absorption spectrum of the transitions $0 \rightarrow n$, $n = 1, 2, \dots, 7$. The transition rates $w_{0,n}$ (in dimensionless units), which are proportional to $\omega_{0n}^4 |\langle \psi_0 | x | \psi_n \rangle|^2$, are plotted versus the resonant light photon energy $\hbar\omega_{0n} = \epsilon_n - \epsilon_0$ in dimensionless units.

In order to compute w_{mn} we still need to know \mathcal{E}_x and compute the energy $e\mathcal{E}_x d$ for these values of d and \mathcal{E}_x . In the absence of an external magnetic field, we can use $d = L$, where $2L$ is the width of the square well. In the presence of a magnetic field, we can use $d = \ell$, the magnetic length. In this case, the dimensionless width of the square well is $2L/\ell$. The relevant energies can be inferred by noting that for a magnetic field of 1 T, $\ell \approx 25$ nm and $\hbar v_F/\ell \approx 21.875$ meV.

[1] Y. Avishai and Y. B. Band, “Klein Bound States in Single-Layer Graphene”, Main Text.

[2] Y. B. Band and Y. Avishai, *Quantum Mechanics with Application to Nanotechnology and Information Science*, Elsevier (2013).